International Core Journal of Engineering Volume 11 Issue 4, 2025
ISSN: 2414-1895 DOI: 10.6919/ICJE.202504_11(4).0054

Crucible Rotation Speed Control Strategy of Czochralski Single Crystal Furnace based on Linear Active Disturbance Rejection Control

Kaiming Yang[1], Xiaotao Chen[1], Dedong Gao[2]

[1] School of Energy and Electrical Engineering, Qinghai University, Xining 810016, China

[2] School of Mechanical Engineering, Qinghai University, Xining 810016, China

Abstract

Aiming at the problems of nonlinearity, strong coupling and interference suppression in the crucible speed control of Czochralski single crystal furnace, this paper proposes a crucible speed control strategy based on Linear Active Disturbance Rejection Control (LADRC). By constructing an extended state observer (ESO) and a nonlinear state error feedback (NLSEF), the real-time estimation and dynamic compensation of the internal and external disturbances of the system are realized, and the problem of insufficient anti-disturbance ability of traditional PID control is solved. Simulation and experiments show that compared with the conventional PID control, the proposed method reduces the overshoot by 13.2 % and the adjustment time by 48.5 % in the step response. It can effectively suppress the influence of temperature fluctuation, mechanical vibration and other interference factors on the speed stability during crystal growth. The research results provide effective control method support for improving the quality of large diameter single crystal.

Keywords

Czochralski Single Crystal Furnace; PID; Active Disturbance Rejection Control; Crucible Speed Control.

1. Introduction

At present, the development potential of the global photovoltaic industry is significant, and the driving force behind it is mainly due to global climate change and the common pursuit of countries to reduce greenhouse gas emissions and achieve the goal of " double carbon. " Under the guidance of these macro policies, photovoltaic development at the technical level is also increasingly evolving to the forefront[1]. In the current photovoltaic power generation system, silicon-based solar cells dominate with its mature manufacturing process and stable performance. Among them, single crystal silicon cells have shown significant advantages in technical iteration due to their excellent low attenuation characteristics and higher photoelectric conversion efficiency[2,3]. Although there are many methods to grow single crystal silicon, there are only two methods commonly used in production[4], namely the Float Zone Process (FZ) method and the Czochralski (CZ) method. Due to the maturity of Czochralski technology, most silicon wafer materials used in integrated circuits are prepared by Czochralski method, which is called CZ monocrystalline silicon[5-6].

Czochralski single crystal furnace is the core equipment for the production of monocrystalline silicon cells. In order to continuously improve the yield and quality of crystal rods, after years of accumulation, the mechanical structure transformation of single crystal furnace has reached a relatively mature level[7-8]. On this basis, in order to further improve the efficiency of crystal pulling and reduce the cost of crystal pulling, it is necessary to optimize the control. Therefore, Winkler. J[9]

ISSN: 2414-1895 DOI: 10.6919/ICJE.202504_11(4).0054

et al. obtained the control method of diameter through speed adjustment through analysis and modeling by observing the meniscus around the crystal rod during crystal pulling. Li [10] et al. analyzed the reactive disturbance of single crystal silicon and concluded that single crystal furnace is a complex system with nonlinear and strong coupling, which is easily affected by external factors[11]. The existing crucible speed control usually adopts PID control. Hu [12] et al. used simulation method to determine the characteristics of the control object through the two-point crossover method, and obtained a set of rules about PID parameter tuning. But the PID control has a large overshoot when controlling the crucible speed, and it is difficult to ensure the control effect when encountering interference.

ADRC technology can estimate and compensate the total disturbance, and has simple structure and strong robustness. It is an effective means to solve nonlinear, coupled, time-varying and uncertain systems [13-16]. Through continuous in-depth research on ADRC, Professor Gao proposed linear ADRC[17-18], which linearizes the parameters, greatly reduces the difficulty of parameter adjustment, and also achieves good control effect in practical engineering application. Gao [19] designed a maximum power point tracking controller based on LADRC, which significantly improved the tracking speed of the algorithm and greatly reduced the power oscillation. Even in the case of dramatic changes in the external environment, it can also show good control ability and strong versatility. However, the research on the anti-interference ability of linear active disturbance rejection control in the crucible speed system of Czochralski single crystal furnace is still blank. Therefore, it is urgent to combine the characteristics of the crucible speed control system and use linear active disturbance rejection control to improve its control process.

In summary, in view of the good control effect of linear active disturbance rejection control in solving nonlinear, coupled, time-varying and uncertain systems and the inherent nonlinear and strong coupling characteristics of the crucible speed system. This paper intends to use linear active disturbance rejection control to improve the anti-interference ability of the crucible speed system of Czochralski single crystal furnace, and reduce the stable response time and overshoot of the system. Based on MATLAB Simulink, the simulation model of crucible speed system of Czochralski single crystal furnace is built, and the effectiveness of the proposed control strategy is verified.

2. Establishment of Crucible Rotational Speed System Model of Czochralski Single Crystal Furnace

In the process of single crystal furnace pulling, the pulling speed, crystal rotation speed, crucible rising speed and crucible rotation speed have a great influence on the final crystal quality. Therefore, it is very important to ensure the stability and accuracy of speed control in the pulling process to improve the crystal quality[20].

In the process of crystal pulling, the crucible rotation is driven by the driving motor to provide the driving force for the crucible. When choosing the motor that drives the crucible rotation, there are generally several requirements. The first is to be light in weight and small in size. The second is to be able to work continuously at low speed and run smoothly. At the same time, it is also required that there is no vibration during its operation. Generally, DC servo motors are mostly used in industrial production. The DC motor has the advantages of small size, high efficiency and convenient control, which is suitable for providing driving force for crucible rotation. DC servo motors have different control methods in different application scenarios. This paper intends to control and optimize the crucible speed, so speed control is adopted. At the same time, due to the low speed of the crucible, no intermediate transmission part is needed, and the crucible is directly driven by the motor. The equation to be satisfied during the operation of the motor is :

Voltage balance equation:

ISSN: 2414-1895 DOI: 10.6919/ICJE.202504_11(4).0054

$$U = K_e \frac{d\theta_m}{dt} + IR_d + L_a \frac{dI}{dt} \tag{1}$$

Torque balance equation:

$$T_m(t) = J_l \frac{d\omega_l}{dt} + K(\theta_m - \theta) + K_i \frac{d\theta_m}{dt} \tag{2}$$

Electromagnetic torque equation:

$$T_m = K_i \tag{3}$$

Load end equation:

$$J_l \frac{d\omega l}{dt} = T_l - b\omega_l \tag{4}$$

$$J_l \frac{d\omega l}{dt} = T_l - b\omega_l \tag{5}$$

In the formula: U is the rated voltage; I Is the rated current; K_e Is the back electromotive force coefficient of the motor; K_i Is the motor torque coefficient; L_a Is an armature inductance; R_a Is an armature resistance; J_m Is the moment of inertia of the motor; J_i Is the moment of inertia of the load; T_m Is the electromagnetic torque of the motor; T_i Is the output torque of the load; θ_m Is the Angle of the motor; θ_i Is the Angle of the load; b Is the viscous friction coefficient.

The intermediate variables are eliminated simultaneously and the Laplace transform is performed. Let, $J = J_m + J_i$,the expression of the motor transfer function is :

$$G(s) = \frac{K_i}{(L_a s + R_a)(Js + b) + K_i K_e} \tag{6}$$

3. Active Disturbance Rejection Control

3.1 Linear Active Disturbance Rejection Control

Nonlinear active disturbance rejection control includes three parts : nonlinear tracking differentiator (TD), extended state observer (ESO) and nonlinear state error feedback (NLSEF). Linear Active Disturbance Rejection Control[17]technology is to replace the nonlinear function of ESO with linearity to obtain a linear extended state observer (LESO), and to replace the nonlinear state error feedback law with a linear state error feedback law (LSEF). The block diagram is shown in Figure 1.

ISSN: 2414-1895 DOI: 10.6919/ICJE.202504_11(4).0054

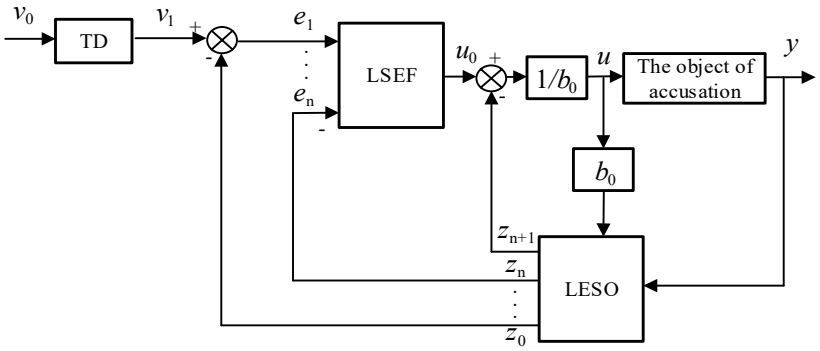

Figure 1. Block diagram of linear active disturbance rejection control

3.1.1 Design of Tracking Differentiator

The function of the tracking differentiator TD is to track the given input signal v0 to obtain its tracking signal v1. Use TD can soften the change of the input signal, ease the contradiction between quickness and overshoot in the process of transition, and enhance the robustness of the controller.

3.1.2 Design of Linear Extended State Observer

The key of LESO is to estimate the sum of the internal and external disturbances of the system while obtaining the estimated value of the state variables of the plant, and obtain the observed quantity of the system disturbances. As shown in Figure 2, According to the control signal u and the measurement signal y of the system output, the linear extended state observer estimates the state variables z_1,... . z_n as well as the real-time action of the total disturbance z_{n+1}, which makes the ADRC controller no longer particularly dependent on the exact model of the system, and the robustness is greatly improved.

Consider an object of order n:

$$y^{(n)} = f(t, y, \cdots, y^{(n-1)}, u, \cdots, u^{(n-1)}, w) + bu \tag{7}$$

In the formula, u and y are the input and output of the system respectively; $y^{(n)}$ is the NTH derivative of y; $u^{(n-1)}$ and $y(n-1)$ are $n-1$ derivatives of u and y, respectively. w is external disturbance; $f(t, y, \cdots, y(n-1), u, \cdots, u(n-1), w)$ (abbreviated f) contains external disturbances of the system and all uncertain factors; b is the given nonzero constant.

The key to the problem lies in the estimation and compensation of f, let f be differentiable and $f' = h$, introduce the extended state $x=[x_1\ x_2\ \ldots\ x_{n+1}]^T$, where $x_{n+1}=f(t, y, \cdots, y^{(n-1)}, u, \cdots, u^{(n-1)}, w)$, the equation (7) can be written as a state space form, That is:

$$\begin{cases} \dot{x}_1 = x_2 \\ \dot{x}_2 = x_3 \\ \cdots\cdots \\ \dot{x}_n = x_{n+1} + b_0 u \\ \dot{x}_{n+1} = h \\ y = x_1 \end{cases} \tag{8}$$

In the formula, b_0 is the estimate value of b.

ISSN: 2414-1895 DOI: 10.6919/ICJE.202504_11(4).0054

According to formula (8), the linear expansion state observer is designed as:

$$\begin{cases} \dot{z}_1 = z_2 + \beta_1(y - z_1) \\ \cdots\cdots \\ \dot{z}_n = z_{n+1} + \beta_n(y - z_1) + b_0 u \\ \dot{z}_{n+1} = \beta_{n+1}(y - z_1) \end{cases} \tag{9}$$

In formul-9 β_1, β_2, ..., β_n is a linear parameter; z is the estimated value of the expansion state $x=[x_1\ x_2 \ldots xn+1]T$, $z=[z_1\ z_2 \ldots z_{n+1}]^T$, z_{n+1} is the comprehensive disturbance of the system.

3.2 Design of Linear Extended State Observer

The function of the linear state error feedback law is to form a control quantity by a suitable linear combination of the signals generated in TD and ESO, and then subtract the disturbance part from the control quantity to obtain a pure control quantity without disturbance, so that the control signal of the system is more reasonable and the control accuracy of the controller is improved.

The design of the linear state error feedback law is shown in equation (10). It can be seen that the nonlinear state error feedback law becomes a PD link after linearization, which can greatly reduce the parameters to be tuned.

$$\begin{cases} e_1 = v_1 - z_1 \\ e_2 = -z_2 \\ \cdots\cdots \\ u_0 = k_p(v_1 - z_1) - k_{d1}z_2 - k_{d2}z_3 - \cdots\cdots k_{dn-1}z_n \\ u = (u_0 - z_{n+1})/b_0 \end{cases} \tag{10}$$

Where v_1 is the input signal; e_1 and e_2 are the error and the error's minor Points; k_p,k_{d1},…,k_{dn-1} the PD link gain.

3.3 Design of Speed Loop based on Linear Active Disturbance Rejection Control

According to the above theoretical discussion, the linear active disturbance rejection controller is used to replace the original speed PI control link of the converter, and the disturbance except the power is estimated and compensated as the external disturbance, which can reduce the contradiction of overdrive and fast, make the power quickly track the reference value, reduce fluctuations, and improve the immunity of the system.

Its control strategy is shown in Figure 2:

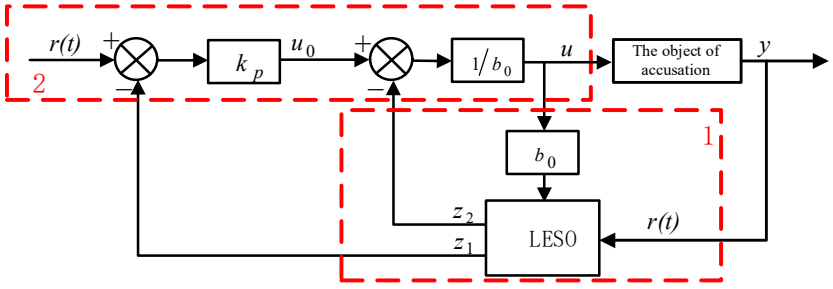

Figure 2. Block diagram of linear active disturbance rejection control

ISSN: 2414-1895 DOI: 10.6919/ICJE.202504_11(4).0054

Due to the rapid action of the system oscillation phenomenon, in order to compensate the system oscillation in a timely and appropriate manner, this paper omits the tracking differentiator link and let v1=r(t). Therefore, the speed control loop based on linear active disturbance rejection control is designed as follows.

(1) Linear expansion state observer

The essence of active disturbance rejection control technology is the design of extended state observer, which tracks the state information and estimates the total disturbance of the system according to the output y of the system and the input u of the controlled object. As shown in dotted line box 1 in Fig.2, the real measured current $r(t)$ is fed back to LESO for state observation.

$$\begin{cases} \dot{z}_1 = z_2 + \beta_1(r(t) - z_1) + b_0 u \\ \dot{z}_2 = \beta_2(r(t) - z_1) \end{cases} \tag{11}$$

The output signals of the observer are z_1 and z_2, the variable z_1 tracks the given instruction signal, and z_2 is the estimate of the total disturbance.

(2) Linear state error feedback law

As shown in the dotted line box 2 in Fig.2, the given speed value $r(t)$ and z_1 are offset and input to LSEF to obtain the output u_0. Then the compensation process is arranged according to the total disturbance estimated by LESO to the feedback control quantity u_0, and the compensated control quantity u is obtained.

Design LSEF is:

$$\begin{cases} u_0 = k_p(r(t)^* - z_1) \\ u = (u_0 - z_2)/b_0 \end{cases} \tag{12}$$

As shown in Fig.2, the above two parts can form a linear ADRC controller.

4. Simulation Verification

Based on MATLAB Simulink simulation platform, this paper simulates and analyzes the crucible speed system of Czochralski single crystal furnace based on LADRC. The relevant parameters of the motor selected in the simulation experiment are K_i=1.38, K_e=14.2, J=0.0023, b=0.0064, R_a=0.9, L_a=3, respectively. Based on MATLAB Simulink simulation platform, this paper simulates and analyzes the crucible speed system of Czochralski single crystal furnace based on LADRC.

According to the transfer function expression obtained above, the relevant parameters of the motor are brought in and the transfer function expression is obtained after unit conversion and calculation:

$$G(s) = \frac{200}{s^2 + 3000s + 2840} \tag{13}$$

It can be concluded from Fig.3 that the adjustment time t_1 of LADRC is 0.16s, the adjustment time t_2 of PID control is 0.33s, and the time for LADRC to reach stability is 0.17 s faster than that of PID control. LADRC control can make the actual output speed reach the theoretical output speed faster

ISSN: 2414-1895 DOI: 10.6919/ICJE.202504_11(4).0054

in the control of the actual crucible speed, which ensures the rapidity of the whole control process. At the same time, the overshoot h_1 of the LADRC is 0, and the overshoot h2 of the PID control is 13.4 %, which realizes no overshoot in the adjustment process. From a qualitative point of view, the LADRC ensures the stability of the control during the pulling process. Especially in the equal diameter stage, it has a great promoting effect on the more stable growth of the crystal rod.

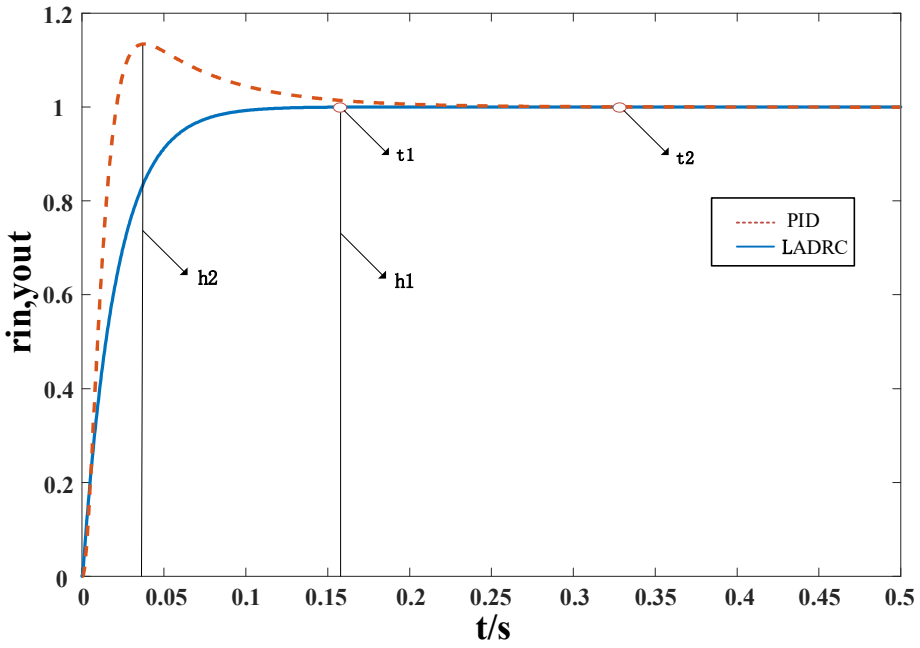

Figure 3. Step response curves under LADRC and PID control

When the simulation time T is 5s, the step interference is added to the system. As shown in Figure 4, the speed offset is 2.8 % under the LADRC, and the speed offset is 14 % under the PID control. The speed offset is relatively reduced under LADRC. Therefore, the control strategy proposed in this paper improves the anti-interference ability of the crucible speed system of the Czochralski single crystal furnace.

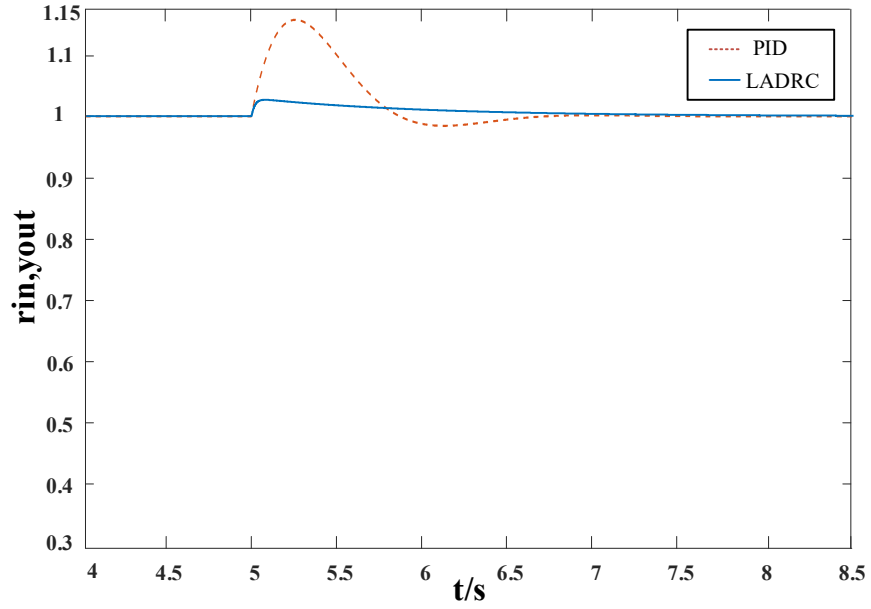

Figure 4. Anti-interference effect diagram of the system under step interference

ISSN: 2414-1895 DOI: 10.6919/ICJE.202504_11(4).0054

5. Conclusion

In this paper, a dynamic simulation model of crucible speed system of Czochralski single crystal furnace is established, and a control strategy of crucible speed based on linear active disturbance rejection control is proposed, which provides a theoretical basis for improving the stability and crystal quality of Czochralski single crystal furnace.

(1) In order to prevent the oscillation accident of the crucible rotation speed system of the Czochralski single crystal furnace, the LADRC technology is used to optimize the system, estimate and compensate the total disturbance of the system, and ensure the stability of the crucible rotation speed system.

(2) The effectiveness of the proposed control strategy applied to the crucible speed system of Czochralski single crystal furnace is verified. Compared with the traditional PID control, the time to reach stability is reduced by 0.17s and the speed offset is reduced by 80%, which improves the stability of the system.

(3) Due to the complex environment in Czochralski single crystal furnace and many parameters that need to be controlled, it is still necessary to consider the coupling effect between various factors in future research, coordinate each influencing factor as a whole, and jointly optimize, so as to improve the quality of monocrystalline silicon produced.

Acknowledgments

Science and Technology Department of Yibin Project [grant numbers 2023YG02]; the Major Science and Technology Projects of the Xining Science and Technology Bureau [grant numbers 2022-Z-03 and 2021-Y-01].

References

[1] CAO S W, ZHOU G Q, CAI Q L et al. Review of solar cells: Materials, policy driving mechanisms and application prospects [J]. Journal of Composite Materials,2022,39(05):1847-1858.

[2] ZHANG X, GAO D G, WANG S, et al. [J]. Journal of Intraocular Lenses, 2019,50(8):1552-1561+1574.

[3] WANG D C, ZENG J, CHEN W P. Technology comparison and economic analysis of new high-efficiency photovoltaic modules [J]. Journal of Water Resources and Hydropower Letters, 2023, 44(11): 95-98.

[4] YU S M. Semiconductor silicon materials science. Hunan: Central South University of Technology Press, 1992

[5] WANG L G, RUI Y, SHENG W, et al. Effect mechanism of Crucible speed on flow field and oxygen concentration in semiconductor grade czochralski silicon melt under transverse magnetic field [J]. Journal of Intraocular Crystals,2023,52(09):1641-1650.

[6] FENG X L. Study on solid-liquid phase variation model and numerical Simulation of silicon single crystal growth by Czochralase method [D]. Xi 'an University of Technology,2018.

[7] CAO J W, GAO Y, CHEN Y, et al. Simulation aided hot zone design for faster growth of CZ silicon mono crystals [J]. Rare Metals, 2011, 30(2):155-159.

[8] SMIRNOVA O V, DURNEV N V, SHANDRAKOVA K E, et al. Optimization of furnace design and growth parameters for Si Cz growth Using numerical simulation [J]. Journal of Crystal Growth, 2008, 310:2185-2191.

[9] J. Winkler, M. Neubert, J. Rudolph. Nonlinear model-based control of the Czochralski process I: Motivation, modeling and feedback controller design [J]. Journal of Crystal Growth,2009, 312(7): 1019-1028.

[10] HU W X, YU L I. [J]. Automation of Refining and Chemical Industry,1996(3):30-34.

[11] LI S F, Zhao J Q, DUN X, et al. Reactivity disturbance analysis of HFETR into monocrystalline silicon [J]. Nuclear Power Engineering,2018,39(S2):98 102.

ISSN: 2414-1895 DOI: 10.6919/ICJE.202504_11(4).0054

[12] PENG X X, WANG S, XU S Z, et al. Diameter Prediction of Czochralski Silicon Single Crystal with Equal Diameter Based on Fuzzy Neural Network [C]. 2022 4th International Conference on Power and Energy Technology (ICPET), 2022.

[13] HAN J Q. Active disturbance rejection control technology [J]. Frontiers in Science, 2007(1): 24-31.

[14] XIE H R, HU C F, LU M, et al. Research on Speed Control Strategy for Permanent Magnet Linear Synchronous Motor Based on Cascaded Linear-Nonlinear Active Disturbance Rejection Controller [J]. Proceedings of the CSEE, 2023: 1-11.

[15] WANG Y, JIANG H H, XING P X. Auxiliary frequency regulation algorithm for grid-connected inverter with auto-disturbance rejection control in stand-alone micro-grid [J]. Electric Machines and Control, 2019, 23(04): 8-19.

[16] ZHAO X, GUO K l, LÜ J J, et al. The Frequency Support Technology Based on Linear Active Disturbance Rejection VSG Control in the Islanding Mode [J]. Power System and Clean Energy, 2023, 39 (07): 17-26.

[17] GAO Z Q. Scaling and bandwidth- parameterization based controller tuning [C]//Proceedings of the American Control Conference, Denver, USA, 2003: 4989-4996

[18] GAO Z Q. The heritage and development of Active Disturbance Rejection Controller [J]. Control Theory & Applications, 2018, 46(15): 52-59.

[19] GAO Z Q, LI S, ZHOU X S, et al. Design of MPPT controller for photovoltaic generation system based on LADRC [J]. Power System Protection and Control, 2018, 46(15): 52-59.

[20] WANG W, HUANG M, CHANG X Y, et al. Research on eccentric balance of lifting System of improved single crystal Furnace [J]. Journal of Intraocular Crystals,2021,50(9):1774-1779.